Arctic Science

OPEN ACCESS | Research Article

Influence of tundra fire severity on vegetation recovery in the Northwest Territories

Angel Chen and Trevor C. Lantz

School of Environmental Studies, University of Victoria, Victoria, BC, Canada

Corresponding author: **Trevor C. Lantz** (email: tlantz@uvic.ca)

Abstract

Anthropogenic climate change has driven an increase in the frequency, size, and severity of fires at high latitudes. Recent research shows that increasing fire severity in the subarctic is altering the trajectories of forest succession, but to date, research on the effect of fire severity on tundra succession has been limited. In this study, we investigated short-term recovery of shrub tundra communities following fire in the Tuktoyaktuk Coastal Plain and Anderson River Plain ecoregions of the Northwest Territories. To understand the effects of fire severity, we documented vegetation and permafrost recovery within moderately burned, severely burned, and unburned portions of six tundra fires that burned in 2012. We found that vegetation structure at moderately and severely burnt sites recovered rapidly toward pre-fire levels, but that differences in community composition, characterized by a decrease in shrub and lichen cover as well as an increase in abundance of ruderals and graminoids, persisted at severely burned sites. The persistence of thermal changes and increased thaw depth indicate that while biotic recovery can occur promptly, severe fire may have long-term impacts on belowground conditions.

Key words: Arctic tundra, fire, vegetation recovery, climate change, vegetation indices

1. Introduction

Over the past half century, the length of the fire season in Canada has increased by approximately 2 weeks and the national trend in annual area burned has increased threefold (Hanes et al. 2019). Fire activity has increased most rapidly in boreal regions of northern Canada (Brown and Johnstone 2011; Walker et al. 2019), where air temperatures are warming at three times the global rate (Vincent et al. 2015; Bush and Lemmen 2019). High-latitude tundra fires have historically been constrained by low biomass, making them less common and severe than boreal forest fires (Wein 1976; Viereck and Schandelmeier 1980). However, warming Arctic temperatures (Vincent et al. 2015) and the proliferation of deciduous shrubs (creating surface fuels) (Ropars and Boudreau 2012*a*; Lantz et al. 2013; Frost and Epstein 2014; Moffat et al. 2016) are projected to increase the probability of fire in the tundra biome by the end of the 21st century (Moritz et al. 2012), and alter the fire return interval from over 800 years to less than 200 years (Higuera et al. 2008; Rocha et al. 2012). In the past half century, Low Arctic tundra regions of Alaska (Sae-Lim et al. 2019; Masrur et al. 2022), Canada (Veraverbeke et al. 2017), and Siberia (Moskovchenko et al. 2020) have seen increases in the number of ignitions, demonstrating that fire regimes are already changing in some areas of the circumpolar north.

In the northern boreal, where spruce forests typically respond to fire by regenerating pre-fire community structure on decadal time scales, high severity fire can favour alternative successional trajectories dominated by deciduous trees (Johnstone and Chapin 2006; Johnstone et al. 2010, 2020; Hollingsworth et al. 2013; Baltzer et al. 2021). In tundra ecosystems, it is possible that climate-driven increases in fire severity will also facilitate alternate successional trajectories (Heim et al. 2021; Jandt et al. 2021; Miller et al. 2023), but additional research is needed to assess the influence of fire severity on recovery, and to characterize post-fire succession (Frost et al. 2020; Gaglioti et al. 2021; Hollingsworth et al. 2021).

Most research in tundra ecosystems indicates that vegetation structure can recover quickly following fire. In Alaska, tussock tundra ecosystems approach pre-fire vegetation cover levels within 5–10 years (Racine et al. 2004; Jones et al. 2009; Bret-Harte et al. 2013), while shrub tundra ecosystems typically require several decades to recover (Lantz et al. 2010; Jones et al. 2013; Frost et al. 2020; Gaglioti et al. 2021; Heim et al. 2021). Past studies also show that the recovery of community composition is a much slower process with some species or functional groups remaining below pre-fire levels for long periods (Frost et al. 2020; Heim et al. 2022; Miller et al. 2023).

In tussock tundra communities fire typically initiates rapid recovery and dominance of tussock-forming sedges (*Eriophorum vaginatum* L.), but in some cases severe fire can increase shrub abundance (Racine et al. 2004). Studies from the Tuktoyaktuk Coastlands in the Northwest Territories (Lantz et al. 2013; Travers-Smith and Lantz 2020), the Brooks Range in

Alaska (Racine et al. 2004, 2006; Gaglioti et al. 2021; Miller et al. 2023), the Alaska North Slope (Jones et al. 2013), and the Yamalo-Nenets Autonomous Okrug in Siberia (Heim et al. 2022) have also shown that fire can facilitate the landscape-scale proliferation of upright shrubs. In tussock-tundra, the recovery of vascular species is predominantly driven by resprouting of individuals, and seedling establishment and success is typically limited because fire typically does not expose new seedbeds (Gartner et al. 1986; Bret-Harte et al. 2013; Frost et al. 2020). Though the leaves of *E. vaginatum* are destroyed by severe fire, the rhizomes and meristems can survive and resprout rapidly within the moist tussock core, where it is enclosed and protected (Bret-Harte et al. 2013). The belowground stems of deciduous and evergreen shrub species can also survive fire, but the recovery of aboveground biomass following fire in shrub tundra is slower, and does not usually reach or surpass pre-fire conditions until at least a decade after fire (Racine et al. 2004; Narita et al. 2015). Recent research on the Seward Peninsula of Alaska also indicates that more frequent and severe fire can promote the recruitment and persistence of grasses (Hollingsworth et al. 2021).

Identifying how variation in tundra burn severity can affect successional trajectories is critical to understand how increasing tundra fire frequency and severity will impact regional and global ecological processes. Changes to tundra vegetation structure can increase snow depth (Jia et al. 2009) and evapotranspiration (Zhang and Walsh 2006; Swann et al. 2010), and alter wildlife habitat (Jandt et al. 2008; Joly et al. 2009; Gustine et al. 2014; Fauchald et al. 2017). At a circumpolar scale, more widespread boreal and tundra fire is predicted to cause a fourfold increase in fire-driven global carbon flux by 2100 (Mack et al. 2011; Abbott et al. 2016; Walker et al. 2019), with model projections suggesting the relative increase in carbon emissions from tundra fire will be up to two times higher than from boreal fires (Abbott et al. 2016). Permafrost thaw and thermokarst subsidence (Myers-Smith et al. 2008; Jones et al. 2015) can also be triggered by severe fire and can remain evident for decades (Racine et al. 2004; Jafarov et al. 2013; Jones et al. 2015).

To date, most research on multi-year and decadal recovery following tundra fire has focused on individual disturbances (Racine et al. 2004; Frost et al. 2020). To our knowledge, only a few studies have evaluated recovery patterns across gradients of burn severity at multiple fires (Rocha and Shaver 2011; Tsuyuzaki et al. 2017). The objective of this study was to evaluate the recovery of tundra ecosystems to burn severity across a range of spatial scales. Recovery refers to the process by which ecosystems return a pre-disturbed reference state and can be evaluated using a number of indictors (Parker and Wiens 2005; Lotze et al. 2011). In this analysis, we explore three aspects of ecological recovery: (1) structural (total vegetation cover and height), (2) compositional (diversity and abundance of plants), and (3) edaphic (soil chemistry, thaw depth, and ground temperature). To accomplish this, we employed a remotely sensed vegetation index to classify burn severity (Allen and Sorbel 2008) and used plot and Remotely Piloted Aerial System (RPAS) surveys, and Landsat-derived Normalized Differenced Vegetation Index (NDVI) data to measure vegetation structure and community composition, soil conditions and terrain properties at six tundra fires that burned in the Northwest Territories in 2012.

2. Methods

2.1. Study area

We conducted this study within the Tuktoyaktuk Coastal Plain and Anderson River Plain Ecoregions, in the Northwest Territories (Fig. 1). This area is located within the continuous permafrost zone, where soils can be ice-rich, and the rolling landscape is characterized by hummocky uplands and lowlands frequently occupied by polygonal peatlands (Ecosystem Classification Group 2012). These ecoregions span the forest-tundra ecotone with landscapes in the southern part of the study area dominated by tall shrubs (*Salix* spp., *Alnus alnobetula* subsp. *fruticosa* (Ruprecht) Raus, and *Betula glandulosa* Michaux) and scattered spruce woodlands (*Picea glauca* (Moench) Voss (Timoney et al. 1992; Travers-Smith and Lantz 2020)). The northern part of the study area is characterized by dwarf shrub and graminoid dominated tundra (Hernandez 1973; Kokelj et al. 2017). The tundra fires sampled in this study burned primarily in upland areas where vegetation was dominated by shrub tundra communities comprised of tall (*Alnus* spp., *Betula* spp., *Salix* spp.) and dwarf (*Rhododendron* spp., *Empetrum* spp., *Vaccinium* spp.) shrubs and graminoids (*Carex* spp., *Eriophorum* spp., *Calamagrostis* spp., *Arctagrostis* spp.). Although much less common, tussock-dominated patches comprised mainly of *Eriophorum* spp. and other graminoids were also present at these sites.

The regional climate of this area is characterized by long cold winters and short summers (Rampton 1998). Mean annual temperatures (MATs) from 1981 to 2010 in Inuvik and Tuktoyaktuk were −8.2 and −10.1 °C, respectively. Annual precipitation was approximately 240 mm in Inuvik and 160 mm in Tuktoyaktuk (Environment Canada 2018). Between 1926 and 2019, mean annual and mean summer temperature increased by 3.5 °C (0.38 °C/decade) and 1.9 °C (0.20 °C/decade), respectively (Travers-Smith and Lantz 2020). Continuous permafrost in this region is ice rich and thermokarst landforms (thaw slumps, thermokarst lakes, polygonal terrain) are common (Ecosystem Classification Group 2012). Increasing MAT has been observed across all weather stations in the western Canadian Arctic over the past half century (Burn and Kokelj 2009; Vincent et al. 2015) and warming has driven an increase in ground temperatures and thaw depths in receent decades (Burn and Kokelj 2009; Kokelj et al. 2017).

2.2. Site selection

To examine the effects of burn severity on tundra landscapes, we used Landsat false colour imagery to locate and identify six tundra fires that burned in 2012 (Table 1). To map spatial variation in the severity of each fire, we determined the approximate dates of ignition and downloaded pre- and post-fire Landsat scenes, which were used to calculate the Normalized Burn Ratio (NBR) (García and Caselles 1991; Key and Benson 1999) (Appendix A). The NBR is a modified version of the NDVI, which uses the shortwave infrared (SWIR)

Fig. 1. Map of study area showing the area of the six tundra fires examined in this study including: Noell Lake (NL), Sandy Hills (SH), Husky Lakes (HL), Tuktoyaktuk (TK), Crossley Lakes (CL), and Anderson River (AR). The dashed line shows the position of the forest tundra transition as mapped by Timoney et al. (1992). Inset map in the upper right shows the location of the study area in northwestern Canada. This map was created in ArcGIS Pro (version 2.7) using publically available data layers.

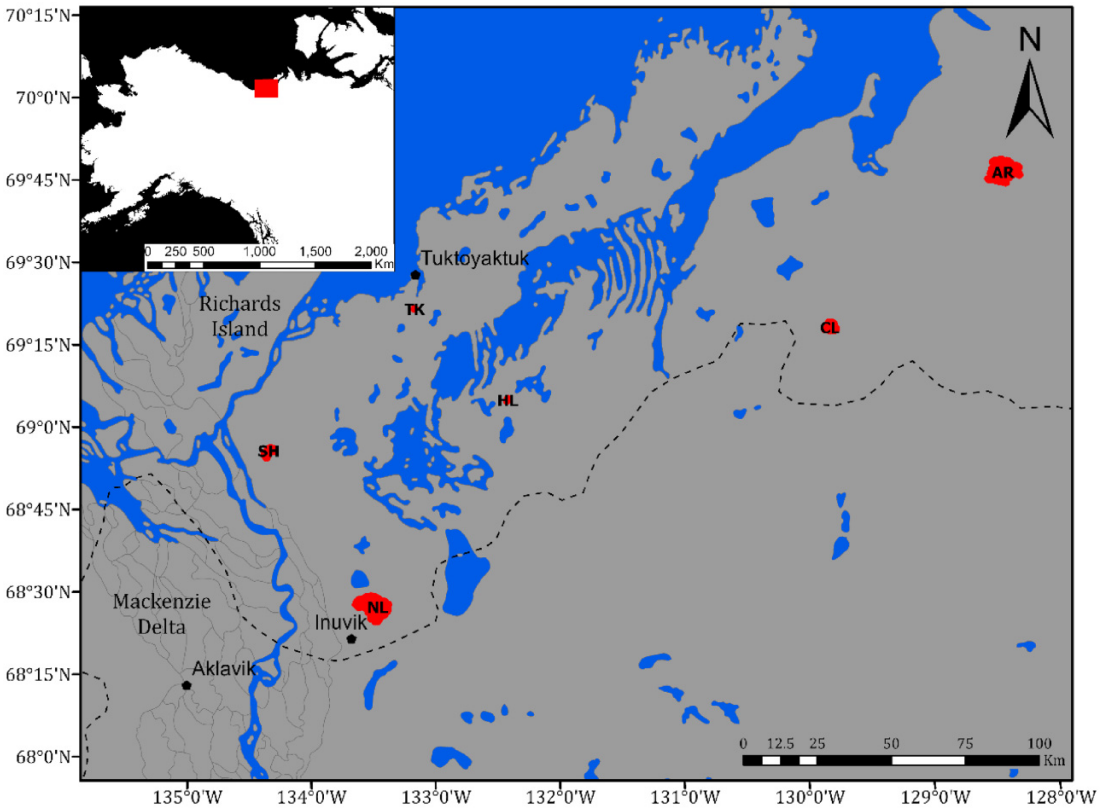

Table 1. Size and estimated timing of the six fires sampled in this study.

Fire name	Size (km^2)	Start date	End date	Pre-fire scene	Post-fire scene
Crossley Lakes (CL)	60.3	24 June 2012	10 July 2012	LT05_L1TP_059012_20110623_20161008_01_T1	LE07_L1TP_060011_20130627_20161124_01_T1
Anderson River (AR)	392.7	24 June 2012	19 July 2012	LE07_L1TP_060011_20110622_20161208_01_T1	LE07_L1TP_060011_20130627_20161124_01_T1
Tuktoyaktuk (TK)	0.63	04 June 2012	20 June 2012	LT05_L1TP_064011_20110626_20161008_01_T1	LE07_L1TP_064011_20130607_20161124_01_T1
Husky Lakes (HL)	3.5	22 June 2012	24 July 2012	LE07_L1TP_062011_20110620_20161208_01_T1	LE07_L1TP_061012_20130618_20161123_01_T1
Sandy Hills (SH)	36.0	27 June 2012	13 July 2012	LT05_L1TP_063012_20110619_20161008_01_T1	LE07_L1TP_065011_20130614_20161123_01_T1
Noell Lake (NL)	53.0	13 June 12	9 August 2012	LT05_L1TP_063012_20110619_20161008_01_T1	LE07_L1TP_061012_20130618_20161123_01_T1

Note: Landsat scenes used to calculate the severity of each fire are shown in the last two columns.

and near infrared (NIR) bands to identify burned areas:

$$\mathrm{NBR} = \frac{\mathrm{NIR} - \mathrm{SWIR}}{\mathrm{NIR} + \mathrm{SWIR}}$$

Unburned vegetation has high NIR reflectance and low SWIR reflectance and burned vegetation has low NIR and high SWIR reflectance (Keeley et al. 2008). Differenced NBR (dNBR) is calculated by subtracting post-fire NBR from pre-fire NBR to estimate burn severity and the magnitude of post-fire surface change (Chen and Huang 2008), with higher values of dNBR indicating higher fire severity. The six fires we studied burned in June 2012 and Landsat scenes for dNBR calculation were selected based on proximity to the anniversary of the burn date pre-fire (June 2011) and post-fire (June 2013) using the method described by Key and Benson (2006). Top of Atmosphere Landsat Thematic Mapper, Enhanced Thematic Mapper Plus (ETM+), and Operational Land Imager (OLI) images were downloaded from the United States Geological Survey Earth Resources Observation and Sciences Center Science

Processing Architecture for fire mapping. Burn severity calculations and classifications were performed in R (R Core Team 2018). To derive gapless dNBR calculations where Landsat images were affected by the Scan Line Corrector failure, OLI reflectance values were transformed and calibrated to correspond with ETM+ values using the "calc" function in the "raster" package in R (Hijmans 2023).

Fire severity classes were delineated by adapting the dNBR thresholds from the US Forest Service's *Fire Effects Monitoring and Inventory System*. Specifically, we defined our severity classes as: (1) unburned (dNBR < 100), (2) moderate severity (dNBR ≥ 100 and <400), and (3) high severity (dNBR ≥ 400) (Appendix B). This approach was designed for forest monitoring in the contiguous United States, but has also been used in northern boreal regions (Epting et al. 2005). We did not apply atmospheric correction to calculations of the NBR, as previous studies have found that the effects of atmospheric scattering are limited in the NIR and SWIR wavelengths used in this calculation (Miller et al. 2009). Atmospheric correction can also introduce errors when using imagery from multiple dates that likely differ in atmospheric effects (Miller et al. 2009; Fang and Yang 2014).

2.3. NDVI trends

To assess vegetation recovery dynamics among severity classes at each fire scar from 1998 to 2018, we used Google Earth Engine to calculate NDVI trends using the Landsat composite time-series application (Braaten 2021). NDVI is a vegetation index strongly related to leaf area and phytomass and commonly used as a proxy for productivity (Riedel et al. 2005; Raynolds et al. 2012). Annual composite surfaces were created from the mean NDVI between July 1 and September 1 for each year between 1998 and 2018. To extract NDVI values, we randomly selected 50 points within each fire severity class (moderately burned, severely burned, and unburned). Unburned areas were at least 10 m beyond the mapped boundary of each fire, and showed no evidence of recent fire, but have likely all burned in the last 200–1000 years. At each of the six fires, this yielded 150 points. These points were used to calculate the mean summer NDVI value for each severity class in each year. A sample size of 50 points per severity class was chosen to adequately capture intra-annual variation in vegetation productivity at the largest of the six fires. Unburned areas were selected in areas that matched pre-burned terrain conditions by inspecting pre-fire Landsat imagery. To express the magnitude of the difference in post-fire NDVI relative to annual variation in NDVI levels in unburned areas, we calculated the annual NDVI Departure by subtracting mean NDVI in unburned areas from mean NDVI in each burned severity class. Negative values of this index indicate that post-fire greenness remains below reference levels and positive values suggest that post-fire NDVI exceeds levels at undisturbed sites.

2.4. RPAS surveying

RPAS surveys were conducted from 3 July to 30 July 2018 at each fire site. We used a DJI Phantom 4 Advanced quadcopter and the built-in camera to fly surveys in unburned, moderately burned, and severely burned regions of each fire site. DJI Ground Station Pro was used to create flight plans that had 80% overlap between successive images (end overlap) and flightlines (side overlap). Surveys were flown at an altitude of 40 m, which yielded a ground resolution of 1.5 cm. Overall, we surveyed between 1–3 patches of approximately 180 m^2 in each severity class at each fire ($n = 32$). Images were shot at 4:3 aspect ratio with an 84° field of view. Markers for ground control points (GCPs) were placed in the southwest corner of the sample plots described in the next section and were used to orthorectify RPAS images. The precise locations of the markers were identified using two Emlid Reach Global Navigation Satellite System receivers. The base receiver logged continuously over the duration of each survey (approximately 2–3 h) and the second receiver was set to log the location of each GCP for 5–10 min. Five GCPs were distributed across each survey, coinciding with sampling plots. Emlid data were processed using RTK Post software suite to derive precise coordinates for each GCP. Imagery from RPAS surveys was processed using Structure-from-Motion photogrammetric image sequencing in Agisoft Photoscan. Orthomosaics were composited for each survey and used to create digital surface models, digital terrain models, and canopy height models using the approach detailed in Fraser et al. (2016). Survey images were orthorectified by manually identifying and placing GCPs for each survey.

2.5. Field sampling

To compare ecological recovery among fires and severity classes, we conducted field sampling from 3 July to 30 July 2018 to describe vegetation structure, community composition, and soil and permafrost conditions within unburned reference areas and moderately and severely burned regions of the six fires mentioned in the previous sections. We measured species abundance, shrub height, thaw depth, electrical conductivity (EC), organic layer depth, and soil moisture at each burned site (table 2.1; fig. 2.1) and unburned reference sites adjacent to each fire. We used randomized stratified sampling to select sites using the dNBR burn severity classes defined above. At each fire we randomly selected two sites in moderately burned areas, two sites in severely burned areas, and two sites in unburned areas outside of the burn perimeter for a total of six sites. All unburned sites were located at least 10 m beyond the perimeter of the fire. At each site of these 36 sites, five sampling plots were randomly selected for a total of 180 plots across the study area. To measure vegetation structure and composition at each plot, we used a nested quadrat approach. A single quadrat with an area of 4 m^2 was used to visually estimate the percent cover of upright shrubs and trees and to measure tree or shrub canopy height using a tape measure. We estimated the percent cover of dwarf shrub, graminoid, herbaceous dicot, and non-vascular species, and the percent litter (dead, unburned plant material) by placing a single 0.25 m^2 quadrat inside the southeast corner of each 4 m^2 quadrat. Percent cover estimates were made by a single observer at the species level, except for graminoids, lichens, and mosses, which were estimated at the family (graminoids) or functional group (mosses

and lichens) level. Species names and authorities follow the Database of Vascular Plants of Canada (Brouillet et al. 2010).

Soil properties including thaw depth, volumetric soil moisture, and organic layer depth were measured at the center and corners of each 4 m^2 quadrat ($n = 5$). Volumetric soil water content was estimated in the field at the top of the mineral soil horizon using a Delta ThetaProbe Soil Moisture Sensor and HH2 moisture meter. Thaw depth was measured by depressing an active layer probe to the depth of refusal. To standardize thaw depth measurements made throughout the thaw season we estimated maximum thaw depth by adding 0.2 cm day^{-1} (Ovenden and Brassard 1989) for measurements made before 1 August. A shovel was used to dig a small hole exposing upper soil layers and a small ruler was used to measure organic depth. At each plot we collected a single soil sample from the center of the plot. These samples, which consisted of the top 10 cm of the soil matrix below the litter and organic horizon, were placed in plastic bags, labeled, and frozen until they were prepared for lab analysis.

To measure air and ground temperature at our sites, we installed thermistors at one severely burned and one unburned control site within each fire ($n = 12$). To measure near surface and top-of-permafrost temperature we drilled shallow boreholes (100 cm) and attached thermistors to a plastic pipe, which was positioned in the borehole at depths of 5 and 100 cm. To measure air temperature thermistors were positioned at 1.5 m above the ground inside RS1 solar radiation shields (Onset Computing Corporation, Pocasset, MA, USA). We used Hobo Pro U23-003 data loggers with our thermistors, which have accuracy and precision of ±0.21 and 0.02 °C. Loggers were set to continuously record measurements every 2 h until downloaded the following summer.

2.6. Lab analysis

In late August 2018, thawed soil samples were homogenized and used to estimate soil moisture and to prepare pore water extracts used to measure the concentration of major ions, conductivity, and pH. Samples were weighed before and after being oven dried at 45 °C for 5–7 days to calculate gravimetric water content as:

$$\frac{\text{Mass of water (g)}}{\text{Mass of oven dry soil (g)}}$$

Samples for pore water extracts were air-dried, passed through a 2 mm sieve and used to create a 1:5 solution of soil to deionized water (He et al. 2012; Klaustermeier et al. 2016). Soil solutions were agitated continuously for 10 s bihourly for a total of 12 h, then left to settle for 12 h, agitated again for 10 s, and centrifuged at 8000 rotations per minute for 30 min. The temperature-corrected EC and pH of the supernatant were measured using an ExStik PH100 pH meter (Extech Instruments, Waltham, MA, USA) and a TDSTestr 3 conductivity meter (Oakton Instruments, Vernon Hills, IL, USA). After pH and EC were measured, we filtered the supernatant using 45 μm syringe filters, placed the samples into vials, and shipped them to Taiga Labs in Yellowknife, NT for major ion analysis using Inductively Coupled Plasma Mass Spectrometry.

2.7. Data analysis

To assess differences in community composition among severity classes, we conducted a non-metric multidimensional scaling (NMDS) ordination using the "vegan" package (Oksanen et al. 2024) in R. NMDS is an ordination technique that helps to visualize differences in multivariate species composition data. A matrix of species and functional group cover data was log (x + 1) transformed prior to calculating a Bray–Curtis distance matrix used in the ordination plots. We visualized differences in community composition among severity classes with ordination plots and used the envfit and bioenv functions in vegan to test for significant relationships among environmental variables and NMDS scores. An Analysis of Similarity (ANOSIM) (Clarke and Gorley 2001) was performed to test for significant differences in community composition among severity classes (severe burn, moderate burn, and unburned). This analysis is similar to a one-way Analysis of variance (ANOVA), but uses ranked Bray–Curtis dissimilarities to test for significant differences in species composition between groups (Legendre and Legendre 1998). The null hypothesis of our ANOSIM was that there is no difference in average rank dissimilarity between severity classes. The R_{ANOSIM} statistic produced by this analysis provides a measure of dissimilarity between site types; with values close to zero indicating similarity in species composition and values close to 1 indicating complete lack of overlap in species composition (Clarke and Gorley 2001). To identify the species that made the largest contribution to dissimilarity between severity classes we used the SIMPER (similarity percentage) function. This analysis calculates the percent contribution of each species to the Bray–Curtis distances among pairs of site types (Clarke and Gorley 2001).

To test for significant differences in RPAS-derived canopy height estimates among severity classes within a fire we used the lme4 package in R to construct mixed model ANOVAs, which treated fire severity as a fixed effect and sample plots (RPAS surveys) within each fire as a nested random effect (Bates et al. 2015). To ensure that models were consistent with the assumptions of linear mixed effects modeling, we used the DHARMa-package to generate plots of fitted versus residual values.

3. Results

3.1. Landscape scale responses (Landsat and RPAS analyses)

NDVI data from 2013 to 2018 show that vegetation at all fires showed increased productivity during the first 6 years following fire (Fig. 2). Pre-fire NDVI departures were similar among most severity classes and study fires indicating that burned sites were similar to reference sites before fire. During the year of burn NDVI departures declined rapidly (Fig. 2). After the initial decline, moderately burned sites showed rapid increases in NDVI departure, and were typically closer to NDVI values at nearby unburned sites than at severely burned areas. In severely burned areas at four sites (Anderson River, Crossley Lakes, Husky Lakes, and Noell Lake) post-fire NDVI departures remained below pre-fire levels after 6

Fig. 2. Departure in the average Normalized Differenced Vegetation Index (NDVI) in moderately and severely burned areas of six tundra fires. NDVI Departure was calculated by subtracting the mean of a random sample of 50 points in an adjacent unburned area from the mean of a random sample of 50 points from within each severity class at each fire. The dashed vertical line shows the year of fire (2012) and the points to the left of this line show pre-fire NDVI Departure from 1998 to 2011.

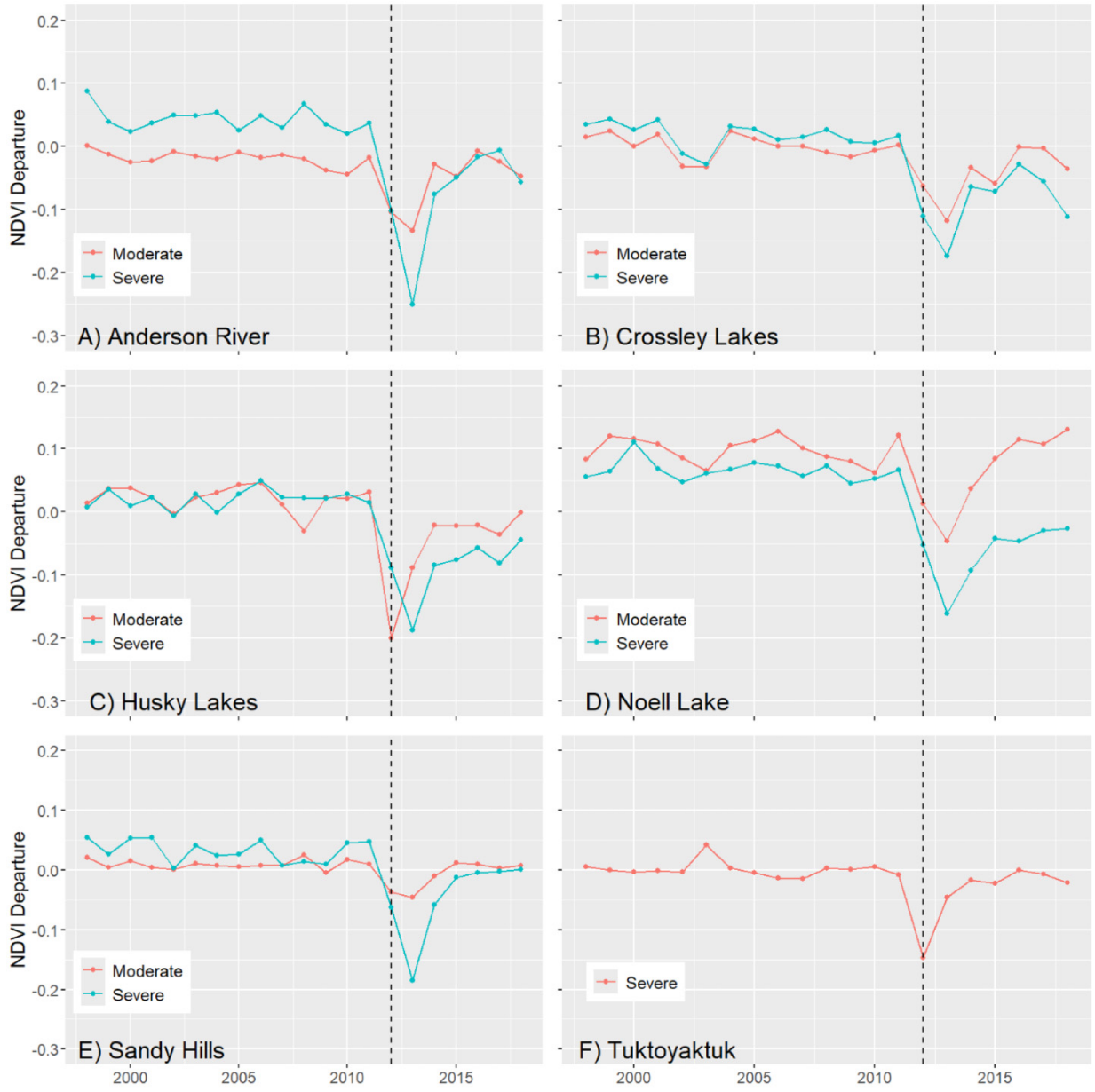

years (Fig. 2). NDVI departures at the Anderson River site also indicate that more severely burned sites were more productive pre-fire compared to moderately burned sites. Although canopy height was elevated in burned areas compared to controls at several sites (Noell Lake and Sandy Hills), a mixed model ANOVA revealed that there were no significant differences in canopy height between severity classes (Fig. 4).

3.2. Field-based responses

Field measurements revealed that community composition also showed significant recovery six years post-fire (Fig. 3A). A one-way ANOSIM showed that plant community composition at moderate and unburned control sites ($R_{ANOSIM} = 0.063$) and moderate and severely burn sites ($R_{ANOSIM} = 0.083$) could not be clearly distinguished. Plant community composition at severely burned sites was moderately distinct from unburned control sites ($R_{ANOSIM} = 0.221$). Differences in plant community composition between severely burned sites and controls were driven by lower abundance of deciduous and evergreen shrubs and lichen and an increase in the cover of bryophytes, grasses (Poaceae), mosses and litter at severely burned sites (Table 2; Fig. 3B). Areas impacted by high severity fire were also characterized by increased abundance of ruderals (*Chamaenerion angustifolium* (L.) Scopoli, and *Tephroseris palustris* (L.) Reichenbach) and graminoids (*Carex* spp., Poaceae spp.) and decreased cover of shrubs (*B. glandulosa*, *V. vitis-idaea*

Fig. 3. Non-metric multidimensional scaling (NMDS) ordination plot of plant community composition based on Bray–Curtis dissimilarity. Points represent sample plots and are coloured by burn severity class. Vectors in the upper panel (A) show correlations between edaphic variables and NMDS scores. Vectors in the lower panel (B) show correlations between percent cover of individual species or species groups and NMDS scores. CHM is canopy height model and NBR is the differenced Normalized Burn Ratio. The NMDS ordination had a final stress of 0.22 after 50 iterations. Clarke and Warwick (2001) state a stress around 0.2 to be within the range for useful 2D interpretations.

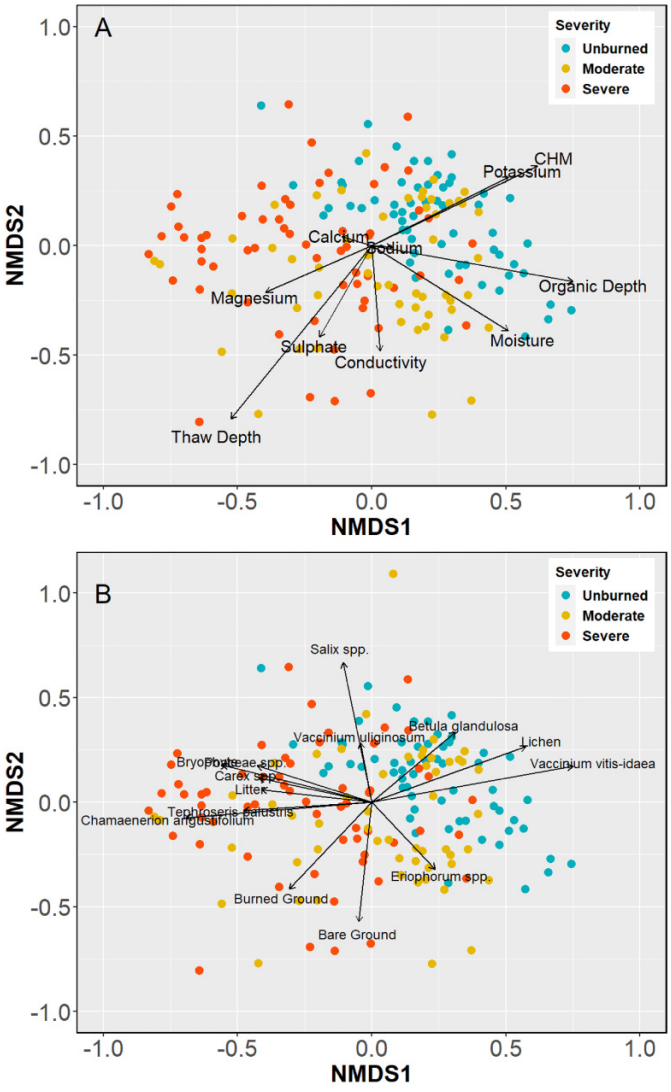

L.) and lichen (Fig. 3B). Unburned sites were typically dominated by deciduous (*Betula glandulosa*, *Vaccinium uliginosum* L., *Salix* spp.) and evergreen (*Empetrum nigrum*, *Vaccinium vitis-idaea*) shrubs, and sedges (*Carex* spp., *Eriophorum* spp.) and grasses (Poaceae) (Table 2; Fig. 3B). Our multivariate analysis showed that higher fire severity was associated with increased thaw depth and micronutrient concentration ($SO4^{-}$, Mg^{2+}) and decreased organic depth (Fig. 3A).

Indicators of disturbance such as bare ground and remnants of burned vegetation persisted in moderately burned and severely burned sites 6 years after fire (Fig. 3). Bare ground was observed in 47 out of 80 burned sites but only 3 out of 40 unburned sites.

Average soil temperature at 5 cm below the surface was generally higher at severely burned sites compared to unburned control sites (Fig. 5A). This difference was largest in late June, when average temperature across severely burned sites was up to approximately 1.2 °C higher than adjacent unburned control sites (Fig. 5A). Severely burned sites also exhibited an early increase in spring temperature at the ground surface and the top of permafrost compared to controls (Fig. 5). Differences in soil temperatures between burned and unburned sites were also apparent at 1 m below the surface during the early winter (Fig. 5B). The date of freezeback at severely burned sites was between 2 weeks and 3 months later compared to unburned controls (Table 3).

4. Discussion

Our multiscale analysis shows that shrub tundra vegetation structure recovers within 6 years following fire, but suggests that community composition remains distinct on decadal scales. Remotely sensed NDVI trends and estimates of canopy height revealed that most study sites returned to pre-fire levels within 6 years following fire (Figs 2 and 4). This is consistent with previous tundra fire recovery studies showing that aboveground primary productivity returns to pre-fire levels a few years after moderate and severe burning (Racine et al. 2004; Bret-Harte et al. 2013; Yeung and Li 2018). Past studies have shown that rapid recovery is driven by the expansion of near-surface buds, a common life-history strategy for tundra species, following disturbance (Wein et al. 1973; Bret-Harte et al. 2013; Yeung and Li 2018).

Our observation that the recovery of shrubs, and lichens was more limited is also consistent with previous research showing that the recovery of these functional groups can take decades (Vavrek et al. 1999; Racine et al. 2006; Jandt et al. 2008; Jones et al. 2013; Gaglioti et al. 2021; Heim et al. 2022). Although shrub cover at our sites had not returned to pre-fire levels 6 years following fire, moderate cover of shrubs from vigorous re-sprouting of *Betula glandulosa* suggests that shrubs are likely to return to pre-fire levels in several years. Aboveground biomass of deciduous shrubs such as *Betula glandulosa* and *Vaccinium uliginosum* is typically destroyed by fire, but can recover quickly via re-sprouting and exceed pre-fire levels of abundance (Wein et al. 1973; Dyrness and Norum 1983; Groot and Wein 2004). Sprouting can occur from dormant buds on root crowns and rhizomes (Zasada 1986; Groot 1998) on these species, which facilitates rapid regeneration after fire, even when burning is severe (Groot and Wein 2004).

Previous research in the subarctic, indicates the dominance of herb and graminoid understories in early successional stages after fire can accelerate nutrient cycling, which limits organic layer development and promotes the development of deciduous shrub communities that are better adapted to shallow organic layers (Chapin et al. 1996; Johnstone et al. 2010; Gibson et al. 2016). Tundra shrubs, par-

Table 2. SIMPER analysis showing the top 10 species or species groups with the greatest contribution to Bray–Curtis dissimilarity between burn severity classes.

Site types	Site type 1 abundance (%)	Site type 2 abundance (%)	Dissimilarity	Cumulative dissimilarity (%)
Control and severely burned				
Bryophytes	19.12	36.36	15.76	15.76
Litter	22.82	30.12	12.48	28.24
Betula glandulosa	16.27	11.00	7.7	35.94
Vaccinium vitis-idaea	16.48	6.53	7.59	43.53
Lichen	13.22	2.74	6.93	50.46
Eriophorum spp.	7.12	4.38	5.6	56.06
Rhododendron tomentosum	11.27	6.03	5.49	61.55
Empetrum nigrum	9.53	2.31	5.41	66.96
Poaceae spp.	1.33	7.64	4.77	71.73
Salix spp.	5.63	4.59	3.64	75.37
Moderately burned and severely burned				
Bryophytes	22.05	36.36	16.82	16.82
Litter	25.16	30.12	12.75	29.57
Eriophorum spp.	11.95	4.38	8.08	37.65
Vaccinium vitis-idaea	11.98	6.53	6.79	44.44
Betula glandulosa	12.62	11.00	6.69	51.13
Rhododendron tomentosum	11.55	6.03	6.13	57.26
Poaceae spp.	3.64	7.54	6.02	63.28
Vaccinium uliginosum	2.38	4.66	4.31	67.59
Empetrum nigrum	4.25	2.31	3.63	71.22
Salix spp.	3.33	4.59	3.48	74.70
Control and moderately burned				
Bryophytes	19.12	22.05	12.41	12.41
Litter	22.82	25.16	11.87	24.28
Eriophorum spp.	7.12	11.95	9.18	33.46
Vaccinium vitis-idaea	16.48	11.98	8.49	41.95
Betula glandulosa	16.27	12.62	8.16	50.11
Lichen	13.22	3.91	7.56	57.67
Rhododendron tomentosum	11.27	11.55	6.66	64.33
Empetrum nigrum	9.53	4.25	6.13	70.46
Rubus chamaemorus	3.40	4.44	3.79	74.25
Salix spp.	5.63	3.33	12.41	77.78

Note: Site type 1 and 2 correspond to the sites listed in the pair-wise comparisons noted in the first column. Each comparison group is ordered by the species or species group making the largest contributions to dissimilarity.

Table 3. Date of freezeback (2018-19) at severely burned sites and control in the study area.

Fire	Freezeback—control	Freezeback—severe burn
Tuktoyaktuk	16 September	4 October
Crossley Lake	16 September	21 December
Anderson River	15 September	24 December
Husky Lakes	1 October	8 December
Noell Lake	No data	29 May (2019)
Sandy Hills	No data	29 September

Note: The date of freezeback was defined as the date when ground surface temperatures were 0 °C or below for 3 days in a row and ground temperatures at 100 cm below the ground surface were colder than −0.5 °C.

ticularly *Betula glandulosa*, *Alnus alnobetula* subsp. *fruticosa*, and *Salix* spp., have also shown increased stem biomass, density, and dominance over graminoid species (Racine et al. 2004; Gaglioti et al. 2021) in response to increased thaw depth, pH, and nutrient availability (Ca2+, SO4−) in later successional stages following disturbance (Schuur et al. 2007; Lantz et al. 2009). Greenhouse treatments that increase below and aboveground temperatures also drive similar responses in dwarf birch (Bret-Harte et al. 2001, 2004; Shaver et al. 2001). Previous studies have also shown that tundra disturbances that reduce or remove organic soils can promote the dominance of deciduous shrubs (Landhausser and Wein 1993; Racine et al. 2004; Lantz et al. 2009, 2010, 2022; Johnstone et al. 2010; Gibson et al. 2016). Our observations of community composition and soils in areas where tundra burning was severe show that shrub tundra has been recovering rapidly and suggests

Fig. 4. Boxplots of canopy height data among severity classes at each fire scar based on an Remotely Piloted Aerial System-derived Canopy Height Model. The line shows median canopy height, the box shows the interquartile range, and the whiskers show the 10th and 90th percentiles of samples.

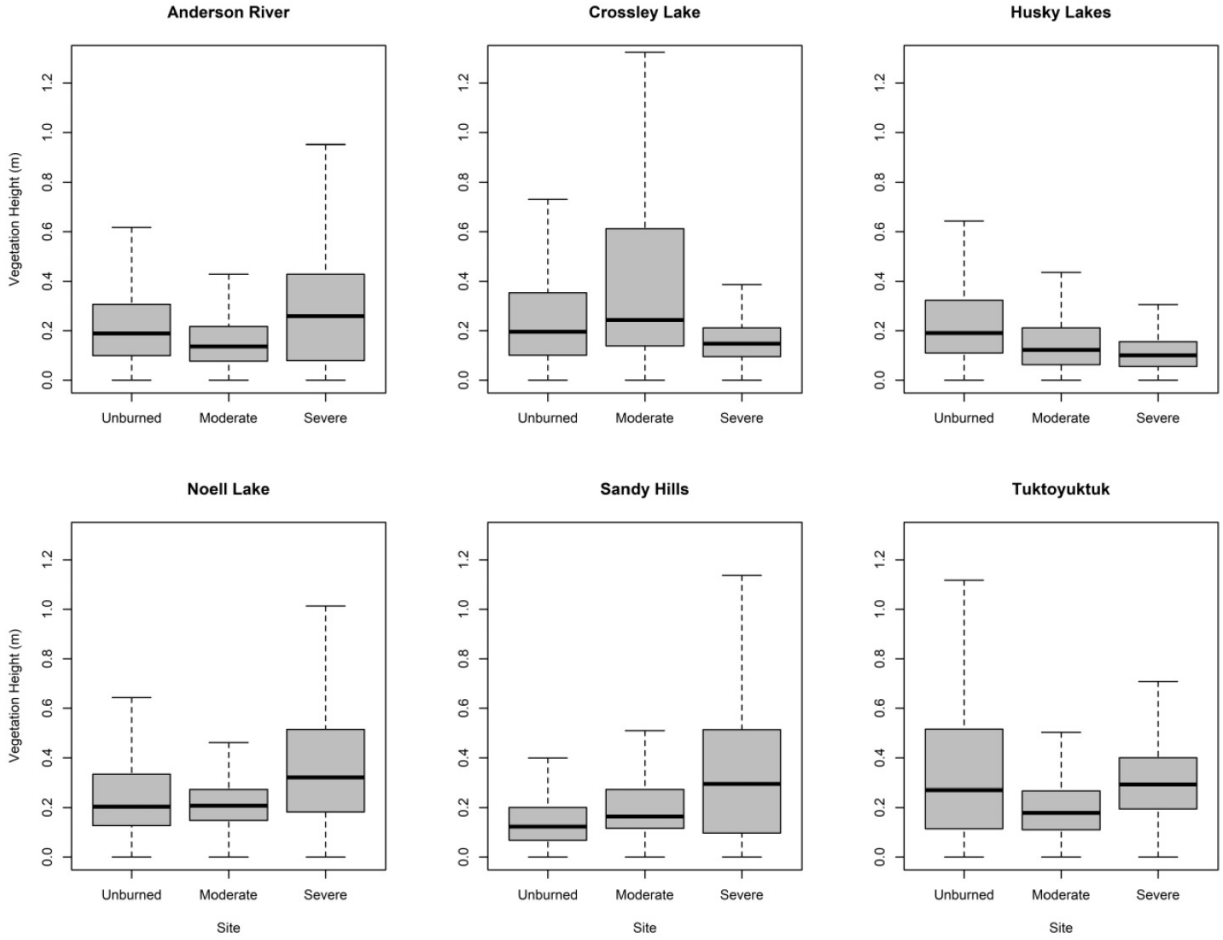

that ongoing succession may promote shrub dominance in a manner similar to observations in other areas (Racine et al. 2004; Higuera et al. 2008; Jones et al. 2009, 2013; Gaglioti et al. 2021; Miller et al. 2023). Ultimately, however, ongoing monitoring is required to track successional change and test this prediction. Future studies in this region should also evaluate recovery trajectories in areas dominated by tussock tundra.

Our observation that changes in community composition and soil conditions were greatest in areas of severe burning indicates that the nature of tundra recovery is a function of disturbance severity. Despite the return of NDVI and canopy height to pre-fire levels, our field sampling showed that recovery of community composition may take longer on severely burned sites. This is likely driven by the success of different regeneration strategies at different fire severities. Deciduous and evergreen shrub cover was comparatively more limited in moderate and severely burned sites than in adjacent unburned sites (Table 2). This is consistent with previous research showing that shrubs are slower to respond than graminoids following fire (Racine 1981; Bret-Harte et al. 2013). Our field sampling suggests that remotely sensed increases in productivity in moderate and severely burned sites were driven primarily by increased abundance of graminoids, which can recover quickly from belowground buds undamaged by fire (Wein et al. 1973; Racine 1981; Gaglioti et al. 2021). Graminoids, as well as several early successional herbs such as *Chamaenerion angustifolium* and *Tephroseris palustris* (Pavek 1992; Lantz et al. 2009; Lantz 2017), recovered rapidly and were common on burned sites 6 years after fire. Although short-term recovery at severely burned sites differed from areas of moderate fire, our observations suggest that the fires scars we sampled were not severe enough to facilitate the development of alternative successional trajectories as has been observed in the subarctic (Landhausser and Wein 1993; Johnstone et al. 2010; Lantz et al. 2010; Hollingsworth et al. 2013).

The persistence of thermal changes 6 years following fire also indicates that severe tundra fire can initiate positive feedbacks that influence abiotic conditions. Higher ground temperatures at severely burned sites can be attributed to increased ground heat flux in the summer (Nossov et al. 2013) following the partial combustion of the soil organic layer. Higher burn severity and the loss of surface cover and organics were also associated with increased thaw depth, and extended thaw season (Fig. 5; Table 3). Increases in thaw depths are noteworthy because they may exacerbate

Fig. 5. Mean daily temperatures measured using thermistors at severely burned sites (red line) and unburned control sites (blue lines) between July 2018 and August 2019. The upper panel (A) shows that the ground surface temperature (5 cm below surface) and the lower panel (B) shows the temperature at the top of permafrost (100 cm below surface).

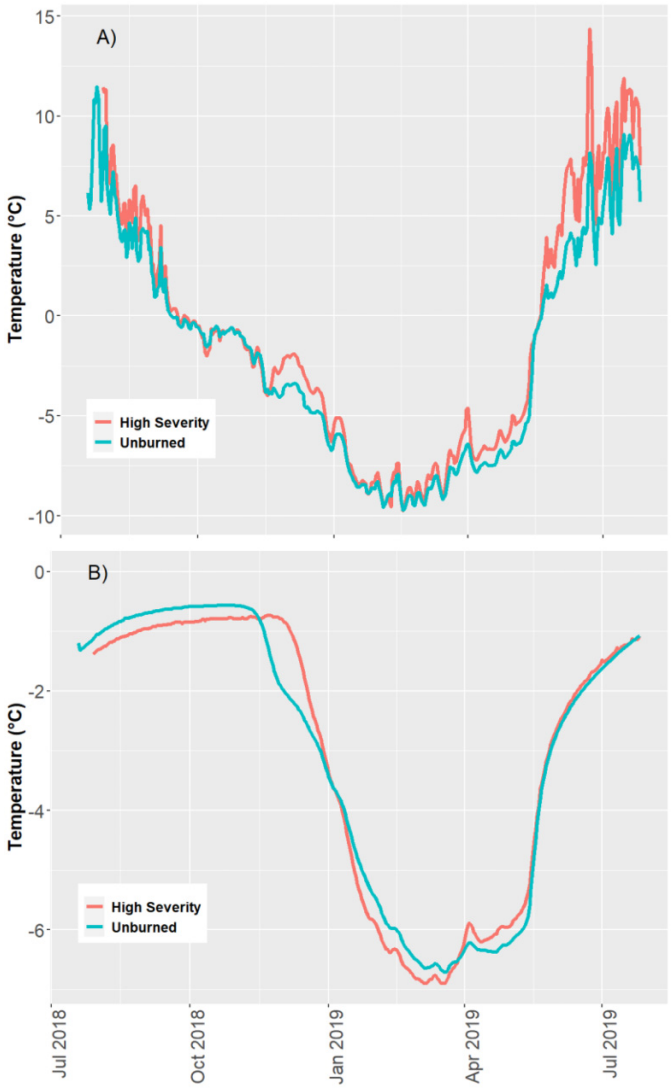

long-term carbon loss by accelerating decomposition rates (Racine et al. 2004; O'Donnell et al. 2011). Thermal recovery can take decades following tundra fire (Jiang et al. 2015), and when the disturbance is severe, it can also facilitate thermal erosion (Chipman and Hu 2017), and thermokarst development (Mackay 1995; Jones et al. 2015) with long-term effects on abiotic conditions. Increased thaw depth at severely burned sites was also associated with higher concentrations of soluble nutrients (SO_4^-, Mg^{2+}), which has been linked to rapid increases in aboveground biomass of deciduous shrubs (Wein et al. 1973; Lantz et al. 2009; Hu et al. 2015).

Predicted decreases in the tundra fire return interval to less than 200 years highlight the importance of understanding post-fire vegetation succession (Young et al. 2017). Many recent studies suggest that increasing burn severity will likely facilitate the expansion of upright shrubs (Lantz et al. 2010, 2013; Jones et al. 2013; Gaglioti et al. 2021; Miller et al. 2023). Palynological studies indicate that during the mid-Holocene shrub tundra landscapes dominated by *Betula glandulosa* burned as frequently as modern black spruce landscapes in the northern boreal (~144 years) (Higuera et al. 2008, 2011). However, some studies indicate that increasing burn severity may lead to the long-term replacement of shrub tundra by graminoid tundra (Higuera et al. 2008, 2011; Barrett et al. 2012; Hollingsworth et al. 2013). It is also possible that an increase in the frequency of fires with a range of severities and differing potential for recruitment from seed will lead to a mosaic of fire-adapted tussock tundra in some areas and the proliferation of upright shrub tundra in others (Gaglioti et al. 2021).

Given the potential impacts of widespread changes in tundra vegetation structure on regional and global ecological processes, such as hydrology (Drake et al. 2019), future fire regimes (Higuera et al. 2008; Gaglioti et al. 2021), global carbon storage (Schuur et al. 2015; Christiansen et al. 2018), permafrost dynamics (Wilcox 1998; Blok et al. 2010), and wildlife habitat (Jandt et al. 2008; Joly et al. 2009) additional research on the long-term effects of tundra fire is critical. The limited availability of reliable data on tundra wildfire has made it difficult to document the effects of severe fire on tundra. Remote sensing and plot-based monitoring should be used to assess how landscapes will change in the decades following disturbance. Fine-scale variation in tundra ecosystems also highlights the importance of using very high spatial resolution data in future research. The emergence of hyperspectral remote sensing and very-high resolution platforms, such as microsatellites and unmanned aerial systems (Fraser et al. 2017), which can quantify high resolution burn severity provides an exciting opportunity to examine landscape-scale successional responses following tundra fire and other disturbances.

Acknowledgements

We would like to thank Joe Antos and Carissa Brown for discussions that informed this research; Mike Newton for his assistance with RPAS data compilation; and Kiyo Campbell, Tracey Proverbs, Jordan Seider, Nicola Shipman, and Hana Travers-Smith for their assistance in the field and their valuable insights throughout this project.

Article information

History dates

Received: 25 November 2022
Accepted: 25 April 2024
Accepted manuscript online: 6 June 2024
Version of record online: 16 August 2024

Copyright

Data availability
Data available upon request.

Author information

Author ORCIDs
Angel Chen https://orcid.org/0000-0002-6079-4258
Trevor C. Lantz https://orcid.org/0000-0001-5643-1537

Author notes
Trevor C. Lantz served as Associate Editor at the time of manuscript review and acceptance and did not handle peer review and editorial decisions regarding this manuscript.

Author contributions
Conceptualization: AC, TCL
Data curation: TCL
Formal analysis: AC, TCL
Funding acquisition: TCL
Investigation: AC, TCL
Methodology: AC
Project administration: TCL
Supervision: TCL
Visualization: AC, TCL
Writing – original draft: AC
Writing – review & editing: AC, TCL

Competing interests
The authors declare there are no competing interests.

Funding information
This research was supported by the Natural Sciences and Engineering Research Council of Canada (Discovery Grant (06210-2018), the Northern Scientific Training Program, the Polar Continental Shelf Program, and the Arctic Institute of North America.

References
Abbott, B.W., Jones, J.B., Schuur, E.A.G., Chapin Iii, F.S., Bowden, W.B., Bret-Harte, M.S., et al. 2016. Biomass offsets little or none of permafrost carbon release from soils, streams, and wildfire: an expert assessment. Environmental Research Letters, **11**: 034014. doi:10.1088/1748-9326/11/3/034014.

Allen, J.L., and Sorbel, B. 2008. Assessing the differenced Normalized Burn Ratio's ability to map burn severity in the boreal forest and tundra ecosystems of Alaska's national parks. International Journal of Wildland Fire, **17**: 463–475. doi:10.1071/WF08034.

Baltzer, J.L., Day, N.J., Walker, X.J., Greene, D., Mack, M.C., Alexander, H.D., et al. 2021. Increasing fire and the decline of fire adapted black spruce in the boreal forest. Proceedings of the National Academy of Sciences, **118**. doi:10.1073/pnas.2024872118.

Barrett, K., Rocha, A.V., Weg, J. Van De, and Shaver, G. 2012. Vegetation shifts observed in Arctic tundra 17 years after fire. Remote Sensing Letters, **3**: 729–736. doi:10.1080/2150704X.2012.676741.

Bates, D., Mächler, M., Bolker, B., and Walker, S. 2015. Fitting Linear Mixed-Effects Models Using lme4. Journal of Statistical Software, **67**: 1–48. doi:10.1101/756163.

Blok, D., Heijmans, M.M.P.D., Schaepman-Strub, G., Kononov, A.V., Maximov, T.C., and Berendse, F. 2010. Shrub expansion may reduce summer permafrost thaw in Siberian tundra. Global Change Biology, **16**: 1296–1305. doi:10.1111/j.1365-2486.2009.02110.x.

Braaten, J. 2021. Landsat Timeseries Explorer. Available from https://jstnbraaten.users.earthengine.app/view/landsat-timeseries-explorer [accessed July, 2023].

Bret-Harte, M.S., Mack, M.C., Shaver, G.R., Huebner, D.C., Johnston, M., Mojica, C.A., et al. 2013. The response of Arctic vegetation and soils following an unusually severe tundra fire. Philosophical Transactions of the Royal Society B: Biological Sciences, **368**: 20120490. doi:10.1098/rstb.2012.0490.

Bret-Harte, S.M., Garcia, E.A., Sacre, V.M., Whorley, J.R., Wagner, J.L., Lippert, S.C., and Chapin, S.F. 2004. Plant and soil responses to neighbour removal and fertilization in Alaskan tussock tundra. Journal of Ecology, **92**: 635–647. doi:10.1111/j.0022-0477.2004.00902.x.

Bret-Harte, S.M., Shaver, G.R., Zoerner, J.P., Johnstone, J.F., Wagner, J.L., Chavez, A.S., IV, et al. 2001. Developmental plasticity allows *Betula nana* to dominate tundra subjected to an altered environment. Ecology, **82**: 18–32. doi:10.1890/0012-9658(2001)082[0018:dpabnt]2.0.co;2.

Brouillet, L., Coursol, F., Meades, S.J., Favreau, M., Anions, M., Bélisle, P., and Desmet, P. 2010. VASCAN, the database of vascular plants of Canada.

Brown, C.D., and Johnstone, J.F. 2011. How does increased fire frequency affect carbon loss from fire? A case study in the northern boreal forest. International Journal of Wildland Fire, **20**: 829. doi:10.1071/WF10113.

Burn, C.R., and Kokelj, S.V. 2009. The environment and permafrost of the Mackenzie Delta area. Permafrost and Periglacial Processes, **20**: 83–105. doi:10.1002/ppp.655.

Bush, E., and Lemmen, D.S. 2019. Canada's Changing Climate Report. Ottawa, ON. Available from https://changingclimate.ca/site/assets/uploads/sites/2/2020/06/CCCR_FULLREPORT-EN-FINAL.pdf [accessed July, 2024].

Chapin, F.S., Bret-Harte, M.S., Hobbie, S.E., and Zhong, H. 1996. Plant functional types as predictors of transient responses of Arctic vegetation to global change. Journal of Vegetation Science, **7**: 347–358. doi:10.2307/3236278.

Chen, X., and Huang, C. 2008. Use of multiple spectral indices to estimate burn severity in the Black Hills of South Dakota. In Proceedings of Pecora 2008.

Chipman, M.L., and Hu, F.S. 2017. Linkages among climate, fire, and thermoerosion in Alaskan Tundra over the past three millennia. Journal of Geophysical Research: Biogeosciences, **122**: 3362–3377. doi:10.1002/2017JG004027.

Christiansen, C.T., Lafreniére, M.J., Henry, G.H.R., and Grogan, P. 2018. Long-term deepened snow promotes tundra evergreen shrub growth and summertime ecosystem net CO2 gain but reduces soil carbon and nutrient pools. Global Change Biology, **24**: 3508–3525. doi:10.1111/gcb.14084.

Clarke, K.R., and Warwick, R.M. 2001. Change in marine communities: an approach to statistical analysis and interpretation. 2nd Ed. Primer-E Ltd, Plymouth, UK.

Clarke, K.R., and Gorley, R.N. 2001. PRIMER v5: user manual. PRIMER-E, Plymouth, United Kingdom.

de Groot, W.J. 1998. Fire ecology of Betula glandulosa Michx. PhD thesis, Department of Renewable Resources, University of Alberta, Edmonton. doi:10.7939/R3CN6Z51D.

Drake, T.W., Holmes, R.M., Zhulidov, A.V., Gurtovaya, T., Raymond, P.A., McClelland, J.W., and Spencer, R.G.M. 2019. Multidecadal climate-induced changes in Arctic tundra lake geochemistry and geomorphology. Limnology and Oceanography, **64**: S179–S191. doi:10.1002/lno.11015.

Dyrness, C.T., and Norum, R.A. 1983. The effects of experimental fires on black spruce forest floors in interior Alaska. Canadian Journal of Forest Research, **13**: 879–893. doi:10.1139/x83-118.

Ecosystem Classification Group. 2012. Ecological regions of the Northwest Territories — Southern Arctic. Department of Environment and Natural Resources, Government of the Northwest Territories, Yellowknife, N.W.T.

Environment Canada. 2018. National climate data and information archive [online]. Available from http://climate.weather.gc.ca/.

Epting, J., Verbyla, D., and Sorbel, B. 2005. Evaluation of remotely sensed indices for assessing burn severity in interior Alaska using Landsat TM and ETM+. Remote Sensing of Environment, **96**: 328–339. doi:10.1016/J.RSE.2005.03.002.

Fang, L., and Yang, J. 2014. Atmospheric effects on the performance and threshold extrapolation of multi-temporal Landsat derived dNBR for burn severity assessment. International Journal of Applied Earth Observation and Geoinformation, **33**: 10–20. doi:10.1016/j.jag.2014.04.017.

Fauchald, P., Park, T., Tømmervik, H., Myneni, R., and Hausner, V.H. 2017. Arctic greening from warming promotes declines in caribou populations. Science Advances, **3**: e1601365. doi:10.1126/sciadv.1601365.

Fraser, R., van der Sluijs, J., and Hall, R. 2017. Calibrating satellite-based indices of burn severity from UAV-derived metrics of a burned boreal forest in NWT, Canada. Remote Sensing, **9**: 279. doi:10.3390/rs9030279.

Fraser, R.H., Olthof, I., Lantz, T.C., and Schmitt, C. 2016. UAV photogrammetry for mapping vegetation in the low-Arctic. Arctic Science, **2**: 79–102. Available from http://www.nrcresearchpress.com. doi:10.1139/as-2016-0008.

Frost, G.V., and Epstein, H.E. 2014. Tall shrub and tree expansion in Siberian tundra ecotones since the 1960s. Global Change Biology, **20**: 1264–1277. doi:10.1111/gcb.12406.

Frost, G.V., Loehman, R.A., Saperstein, L.B., Macander, M.J., Nelson, P.R., Paradis, D.P., and Natali, S.M. 2020. Multi-decadal patterns of vegetation succession after tundra fire on the Yukon-Kuskokwim Delta, Alaska. Institute of Physics Publishing. doi:10.1088/1748-9326/ab5f49.

Gaglioti, B.V., Berner, L.T., Jones, B.M., Orndahl, K.M., Williams, A.P., Andreu-Hayles, L., et al. 2021. Tussocks enduring or shrubs greening: alternate responses to changing fire regimes in the Noatak River Valley, Alaska. Environmental Research Letters, **15(2)**: e2020JG006009. doi:10.1029/2020JG006009.

García, M.J.L., and Caselles, V. 1991. Mapping burns and natural reforestation using Thematic Mapper data. Geocarto International, **6**: 31–37. doi:10.1080/10106049109354290.

Gartner, B.L., Chapin Iii, F.S., and Shavert, G.R. 1986. Reproduction of *Eriophorum* vaginatu by seed in Alaskan Tussock Tundra. The Journal of Ecology, **74**: 1–18. doi:10.2307/2260345.

Gibson, C.M., Turetsky, M.R., Cottenie, K., Kane, E.S., Houle, G., and Kasischke, E.S. 2016. Variation in plant community composition and vegetation carbon pools a decade following a severe fire season in interior Alaska. Journal of Vegetation Science, **27**: 1187–1197. doi:10.1111/jvs.12443.

Groot, W.J. De, and Wein, R.W. 2004. Effects of fire severity and season of burn on *Betula glandulosa* growth dynamics. International Journal of Wildland Fire, **13**: 287–295. doi:10.1071/WF03048.

Gustine, D.D., Brinkman, T.J., Lindgren, M.A., Schmidt, J.I., Rupp, T.S., and Adams, L.G. 2014. Climate-driven effects of fire on winter habitat for Caribou in the Alaskan-Yukon Arctic. PLoS ONE, **9**: e100588. doi:10.1371/journal.pone.0100588. PMID: 24991804.

Hanes, C.C., Wang, X., Jain, P., Parisien, M.-A., Little, J.M., and Flannigan, M.D. 2019. Fire-regime changes in Canada over the last half century. Canadian Journal of Forest Research, **49**: 256–269. doi:10.1139/cjfr-2018-0293.

He, Y., DeSutter, T., Prunty, L., Hopkins, D., Jia, X., and Wysocki, D.A. 2012. Evaluation of 1:5 soil to water extract electrical conductivity methods. Geoderma, **185–186**: 12–17. doi:10.1016/j.geoderma.2012.03.022.

Heim, R.J., Bucharova, A., Brodt, L., Kamp, J., Rieker, D., Soromotin, A.V., et al. 2021. Post-fire vegetation succession in the Siberian subarctic tundra over 45 years. Science of The Total Environment, **760**: 143425. doi:10.1016/J.SCITOTENV.2020.143425. PMID: 33172629.

Heim, R.J., Heim, W., Bültmann, H., Kamp, J., Rieker, D., Yurtaev, A., and Hölzel, N. 2022. Fire disturbance promotes biodiversity of plants, lichens and birds in the Siberian subarctic tundra. Global Change Biology, **28**: 1048–1062. doi:10.1111/gcb.15963.

Hernandez, H. 1973. Natural plant recolonization of surficial disturbances, Tuktoyaktuk Peninsula Region, Northwest Territories. Canadian Journal of Botany, **51**: 2177–2196. doi:10.1139/b73-280.

Higuera, P.E., Brubaker, L.B., Anderson, P.M., Brown, T.A., Kennedy, A.T., and Hu, F.S. 2008. Frequent fires in ancient shrub tundra: implications of paleorecords for Arctic environmental change. PLoS ONE, **3**: e0001744. doi:10.1371/journal.pone.0001744. PMID: 18320025.

Higuera, P.E., Chipman, M.L., Barnes, J.L., Urban, M.A., and Hu, F.S. 2011. Variability of tundra fire regimes in Arctic Alaska: millennial-scale patterns and ecological implications. Ecological Applications, **21**: 3211–3226. doi:10.1890/11-0387.1.

Hijmans, R.J. 2023. raster: Geographic Data Analysis and Modeling_. R package version 3.6-26. Available from https://CRAN.R-project.org/package=raster [accessed July 2023].

Hollingsworth, T.N., Breen, A.L., Hewitt, R.E., and Mack, M.C. 2021. Does fire always accelerate shrub expansion in Arctic tundra? Examining a novel grass-dominated successional trajectory on the Seward Peninsula. Arctic, Antarctic, and Alpine Research, **53**: 93–109. doi:10.1080/15230430.2021.1899562.

Hollingsworth, T.N., Johnstone, J.F., Bernhardt, E.L., and Chapin, F.S. 2013. Fire severity filters regeneration traits to shape Community Assembly in Alaska's Boreal Forest. PLoS ONE, **8**: e56033. doi:10.1371/journal.pone.0056033. PMID: 23418503.

Hu, F.S., Higuera, P.E., Duffy, P., Chipman, M.L., Rocha, A.V., Young, A.M., et al. 2015. Arctic tundra fires: natural variability and responses to climate change. Frontiers in Ecology and the Environment, **13**: 369–377. doi:10.1890/150063.

Jafarov, E.E., Romanovsky, V.E., Genet, H., McGuire, A.D., and Marchenko, S.S. 2013. The effects of fire on the thermal stability of permafrost in lowland and upland black spruce forests of interior Alaska in a changing climate. Environmental Research Letters, **8**: 035030. doi:10.1088/1748-9326/8/3/035030.

Jandt, R.R., Miller, E.A., and Jones, B.M. 2021. Fire Effects 10 Years After the Anaktuvuk River Tundra Fires. BLM Alaska Technical Report #64. Bureau of Land Management; Anchorage, Alaska, USA

Jandt, R., Joly, K., Meyers, C.R., and Racine, C. 2008. Slow recovery of lichen on burned caribou winter range in Alaska tundra: potential influences of climate warming and other disturbance factors. Arctic, Antarctic, and Alpine Research, **40**: 89–95. doi:10.1657/1523-0430(06-122)[JANDT]2.0.CO;2.

Jia, G.J., Epstein, H.E., and Walker, D.A. 2009. Vegetation greening in the Canadian Arctic related to decadal warming. Journal of Environmental Monitoring, **11**: 2231–2238. doi:10.1039/b911677j. PMID: 20024021.

Jiang, Y., Rocha, A.V., O'Donnell, J.A., Drysdale, J.A., Rastetter, E.B., Shaver, G.R., and Zhuang, Q. 2015. Contrasting soil thermal responses to fire in Alaskan tundra and boreal forest. Journal of Geophysical Research: Earth Surface, **120**: 363–378. doi:10.1002/2014JF003180.

Johnstone, J.F., and Chapin, F.S. 2006. Effects of soil burn severity on post-fire tree recruitment in Boreal Forest. Ecosystems, **9**: 14–31. doi:10.1007/s10021-004-0042-x.

Johnstone, J.F., Celis, G., Chapin, F.S., Hollingsworth, T.N., Jean, M., and Mack, M.C. 2020. Factors shaping alternate successional trajectories in burned black spruce forests of Alaska. Ecosphere, **11**. doi:10.1002/ecs2.3129.

Johnstone, J.F., Chapin, S.F., Hollingsworth, T.N., Mack, M.C., Romanovsky, V., and Turetsky, M. 2010. Fire, climate change, and forest resilience in interior alaska1. Canadian Journal of Forest Research, **40**: 1302–1312. doi:10.1139/X10-061.

Joly, K., Jandt, R.R., and Klein, D.R. 2009. Decrease of lichens in Arctic ecosystems: the role of wildfire, caribou, reindeer, competition and climate in north-western Alaska. Polar Research, **28**: 433–442. doi:10.1111/j.1751-8369.2009.00113.x.

Jones, B.M., Breen, A.L., Gaglioti, B.V., Mann, D.H., Rocha, A.V., Grosse, G., et al. 2013. Identification of unrecognized tundra fire events on the north slope of Alaska. Journal of Geophysical Research: Biogeosciences, **118**: 1334–1344. doi:10.1002/jgrg.20113.

Jones, B.M., Grosse, G., Arp, C.D., Miller, E., Liu, L., Hayes, D.J., and Larsen, C.F. 2015. Recent Arctic tundra fire initiates widespread thermokarst development. Scientific Reports, **5**: 15865. doi:10.1038/srep15865.

Jones, B.M., Kolden, C.A., Jandt, R., Abatzoglou, J.T., Urban, F., and Arp, C.D. 2009. Fire behavior, weather, and burn severity of the 2007 Anaktuvuk River Tundra Fire, North Slope, Alaska. Arctic, Antarctic, and Alpine Research, **41**: 309–316. doi:10.1657/1938-4246-41.3.309.

Keeley, J.E., Brennan, T., and Pfaff, A.H. 2008. Fire severity and ecosystem responses following crown fires in California shrublands. Eco-

logical Applications, **18**: 1530–1546. doi:10.1890/07-0836.1. PMID: 18767627.

Key, C.H., and Benson, N.C. 1999. Measuring and remote sensing of burn severity. *In* Proceedings Joint Fire Science Conference and Workshop. Moscow, ID.

Key, C.H., and Benson, N.C. 2006. LA-1 Landscape Assessment (LA) Sampling and Analysis Methods. report # and publisher USDA Forest Service Gen. Tech. Rep. RMRS-GTR-164-CD. Fort Collins, CO, U.S. [accessed July, 2023].

Klaustermeier, A., Tomlinson, H., Daigh, A.L.M., Limb, R., DeSutter, T., and Sedivec, K. 2016. Comparison of soil-to-water suspension ratios for determining electrical conductivity of oil-productionwater-contaminated soils. Canadian Journal of Soil Science, **96**: 233–243. doi:10.1139/cjss-2015-0097.

Kokelj, S.V, Palmer, M.J., Lantz, T.C., and Burn, C.R. 2017. Ground temperatures and permafrost warming from forest to Tundra, Tuktoyaktuk Coastlands and Anderson Plain, NWT, Canada. Permafrost and Periglacial Processes, **28**: 543–551. doi:10.1002/ppp.1934.

Landhausser, S.M., and Wein, R.W. 1993. Postfire vegetation recovery and tree establishment at the Arctic treeline: climate-change-vegetation-response hypotheses. The Journal of Ecology, **81**: 665. doi:10.2307/2261664.

Lantz, T.C. 2017. Vegetation succession and environmental conditions following catastrophic lake drainage in Old Crow Flats, Yukon. Arctic, **70**: 177. doi:10.14430/arctic4646.

Lantz, T.C., Gergel, S.E., and Henry, G.H.R. 2010. Response of green alder (*Alnus viridis* subsp. *fruticosa*) patch dynamics and plant community composition to fire and regional temperature in northwestern Canada. Journal of Biogeography, **37**: 1597–1610. doi:10.1111/j.1365-2699.2010.02317.x.

Lantz, T.C., Kokelj, S.V, Gergel, S.E., and Henry, G.H.R. 2009. Relative impacts of disturbance and temperature: persistent changes in microenvironment and vegetation in retrogressive thaw slumps. Global Change Biology, **15**: 1664–1675. doi:10.1111/j.1365-2486.2009.01917.x.

Lantz, T.C., Marsh, P., and Kokelj, S.V. 2013. Recent shrub proliferation in the Mackenzie Delta uplands and microclimatic implications. Ecosystems, **16**: 47–59. doi:10.1007/s10021-012-9595-2.

Lantz, T.C., Zhang, Y., and Kokelj, S.V. 2022. Impacts of ecological succession and climate warming on permafrost aggradation in drained lake basins of the Tuktoyaktuk Coastlands, Northwest Territories, Canada. Permafrost and Periglacial Processes, **33**: 176–192. doi:10.1002/ppp.2143.

Legendre, P., and Legendre, L. 1998. Numerical Ecology. 2nd ed. Elsevier, Amsterdam.

Lotze, H.K., Coll, M., Magera, A.M., Ward-Paige, C., and Airoldi, L. 2011. Recovery of marine animal populations and ecosystems. Trends in Ecology & Evolution, **26**(11): P595–P605. doi: 10.1016/j.tree.2011.07.008.

Mack, M.C., Bret-Harte, S.M., Hollingsworth, T.N., Jandt, R.R., Schuur, E.A.G., Shaver, G.R., and Verbyla, D.L. 2011. Carbon loss from an unprecedented Arctic tundra wildfire. Nature, **475**: 489–492. doi:10.1038/nature10283. PMID: 21796209.

Mackay, J. 1995. Active layer changes (1968 to 1993) following the Forest-Tundra fire near Inuvik, N.W.T., Canada. Arctic and Alpine Research, **27**: 323–336. Available from http://www.jstor.org/stable/1552025. doi:10.2307/1552025.

Masrur, A., Taylor, A., Harris, L., Barnes, J., and Petrov, A. 2022. Topography, climate and fire history regulate wildfire activity in the Alaskan Tundra. Journal of Geophysical Research: Biogeosciences, **127**. doi:10.1029/2021JG006608.

Miller, E.A., Baughman, C.A., Jones, B.M., and Jandt, R.R. 2024. Biophysical effects of an old tundra fire in the Brooks Range Foothills of Northern Alaska, U.S.A. Polar Science, **39**: 100984. doi:10.1016/j.polar.2023.100984.

Miller, J.D., Knapp, E.E., Key, C.H., Skinner, C.N., Isbell, C.J., Creasy, R.M., and Sherlock, J.W. 2009. Calibration and validation of the relative differenced normalized burn ratio (RdNBR) to three measures of fire severity in the Sierra Nevada and Klamath Mountains, California, USA. Remote Sensing of Environment, **113**: 645–656. doi:10.1016/j.rse.2008.11.009.

Moffat, N.D., Lantz, T.C., Fraser, R.H., and Olthof, I. 2016. Recent vegetation change (1980–2013) in the Tundra ecosystems of the Tuktoyaktuk Coastlands, NWT, Canada. Arctic, Antarctic, and Alpine Research, **48**: 581–597. doi:10.1657/AAAR0015-063.

Moritz, M.A., Parisien, M.-A., Batllori, E., Krawchuk, M.A., Van Dorn, J., Ganz, D.J., and Hayhoe, K. 2012. Climate change and disruptions to global fire activity. Ecosphere, **3**: 1. doi:10.1890/es11-00345.1.

Moskovchenko, D.V., Aref'ev, S.P., Moskovchenko, M.D., and Yurtaev, A.A. 2020. Spatiotemporal analysis of wildfires in the forest Tundra of western Siberia. Contemporary Problems of Ecology, **13**: 193–203. doi:10.1134/S1995425520020092.

Myers-Smith, I.H., Harden, J.W., Wilmking, M., Fuller, C.C., McGuire, A.D., and Chapin, F.S. 2008. Wetland succession in a permafrost collapse: interactions between fire and thermokarst. Biogeosciences, **5**: 1273–1286. doi:10.5194/bg-5-1273-2008.

Narita, K., Harada, K., Saito, K., Sawada, Y., Fukuda, M., and Tsuyuzaki, S. 2015. Vegetation and permafrost thaw depth 10 years after a Tundra Fire in 2002, Seward Peninsula, Alaska. Arctic, Antarctic, and Alpine Research, **47**: 547–559. doi:10.1657/AAAR0013-031.

Nossov, D.R., Jorgenson, M.T., Kielland, K., and Kanevskiy, M.Z. 2013. Edaphic and microclimatic controls over permafrost response to fire in interior Alaska. Environmental Research Letters, **8**: 035013. doi:10.1088/1748-9326/8/3/035013.

O'Donnell, A.J., Boer, M.M., McCaw, W.L., and Grierson, P.F. 2011. Climatic anomalies drive wildfire occurrence and extent in semi-arid shrublands and woodlands of southwest Australia. Ecosphere, **2**: art127. doi:10.1890/ES11-00189.1.

Oksanen, J., Simpson, G. Blanchet, F., Kindt, R., Legendre, P., McGlinn, P., et al. 2024. vegan: community ecology package_. R package version 2.6-6.1. Available from https://CRAN.R-project.org/package=vegan.

Ovenden, L., and Brassard, G.R. 1989. Wetland vegetation near Old Crow, northern Yukon. Canadian Journal of Botany, **67**: 954–960. doi:10.1139/b89-127.

Parker, K.R., and Wiens, J.A. 2005. Assessing recovery following environmental accidents: environmental variation, ecological assumptions, and strategies. Ecological Applications, **15**: 2037–2051. doi:10.1890/04-1723.

Pavek, D.S. 1992. Chamerion angustifolium. In: Fire Effects Information System, [Online]. Fire Sciences Laboratory, U.S. Available from https://www.fs.usda.gov/database/feis/plants/forb/chaang/all.html.

R Core Team. 2018. R: a language and environment for statistical computing. Vienna, Austria.

Racine, C., Allen, J.A., and Dennis, J.G. 2006. Long-term monitoring of vegetation change following tundra fires in Noatak National preserve, Alaska. Programmable.

Racine, C., Jandt, R., Meyers, C., and Dennis, J. 2004. Tundra Fire and vegetation change along a hillslope on the Seward Peninsula, Alaska, U.S.A. Arctic, Antarctic, and Alpine Research Arctic, Antarctic, and Alpine Research, **36**: 1–10. Available from http://www.jstor.org/stable/1552423.

Racine, C.H. 1981. Tundra fire effects on soils and three plant communities along a hill-slope gradient in the Seward Peninsula, Alaska. Arctic, **34**: 71–84. doi:10.14430/arctic2508.

Rampton, V. 1998. Quaternary geology of the Tuktoyaktuk Coastlands, Northwest Territories. Vol. **423**. Geological Survey of Canada, Memoir.

Raynolds, M.K., Walker, D.A., Epstein, H.E., Pinzon, J.E., and Tucker, C.J. 2012. A new estimate of tundra-biome phytomass from trans-Arctic field data and AVHRR NDVI. Remote Sensing Letters, **3**: 403–411. doi:10.1080/01431161.2011.609188.

Riedel, S.M., Epstein, H.E., and Walker, D.A. 2005. Biotic controls over spectral reflectance of Arctic tundra vegetation. International Journal of Remote Sensing, **26**: 2391–2405. doi:10.1080/01431160512331337754.

Rocha, A.V., and Shaver, G.R. 2011. Burn severity influences postfire CO2 exchange in Arctic tundra. Ecological Applications, **21**: 477–489. doi:10.1890/10-0255.1. PMID: 21563578.

Rocha, A.V., Loranty, M.M., Higuera, P.E., MacK, M.C., Hu, F.S., Jones, B.M., et al. 2012. The footprint of Alaskan tundra fires during the past half-century: implications for surface properties and radiative forcing. Environmental Research Letters, **7**: 044039. doi:10.1088/1748-9326/7/4/044039.

Ropars, P., and Boudreau, S. 2012. Shrub expansion at the forest tundra ecotone: spatial heterogeneity linked to local topography. En-

vironmental Research Letters, **7**: 015501. doi:10.1088/1748-9326/7/1/015501.

Sae-Lim, J., Russell, J.M., Vachula, R.S., Holmes, R.M., Mann, P.J., Schade, J.D., and Natali, S.M. 2019. Temperature-controlled tundra fire severity and frequency during the last millennium in the Yukon-Kuskokwim Delta, Alaska. The Holocene, **29**: 1223–1233. doi:10.1177/0959683619838036.

Schuur, E.A.G., Crummer, K.G., Vogel, J.G., and MacK, M.C. 2007. Plant species composition and productivity following permafrost thaw and thermokarst in Alaskan tundra. Ecosystems, **10**: 280–292. doi:10.1007/s10021-007-9024-0.

Schuur, E.A.G., McGuire, A.D., Schädel, C., Grosse, G., Harden, J.W., Hayes, D.J., et al. 2015. Climate change and the permafrost carbon feedback. Nature. doi:10.1038/nature14338.

Shaver, G.R., Bret-Harte, M.S., Jones, M.H., Johnstone, J., Gough, L., Laundre, J., and Chapin, F.S. 2001. Species composition interacts with fertilizer to control long-term change in tundra productivity. Ecology, **82**: 3163–3181. doi:10.1890/0012-9658(2001)082[3163:SCIWFT]2.0.CO;2.

Swann, A.L., Fung, I.Y., Levis, S., Bonan, G.B., and Doney, S.C. 2010. Changes in Arctic vegetation amplify high-latitude warming through the greenhouse effect. Proceedings of the National Academy of Sciences, **107**: 1295–1300. doi:10.1073/pnas.0913846107.

Timoney, K.P., La Roi, G.H., Zoltai, S.C., and Robinson, A.L. 1992. The high subarctic forest-tundra of northwestern Canada: position, width, and vegetation gradients in relation to climate. Arctic, **45**: 1–9. doi:10.14430/arctic1367.

Travers-Smith, H.Z., and Lantz, T.C. 2020. Leading-edge disequilibrium in alder and spruce populations across the forest–tundra ecotone. Ecosphere, **11**. doi:10.1002/ecs2.3118.

Tsuyuzaki, S., Iwahana, G., and Saito, K. 2018. Tundra fire alters vegetation patterns more than the resultant thermokarst. Polar Biology, **41**: 753–761. doi:10.1007/s00300-017-2236-7.

Vavrek, M.C., Fetcher, N., McGraw, J.B., Shaver, G.R., Chapin, F.S., and Bovard, B. 1999. Recovery of productivity and species diversity in tussock tundra following disturbance. Arctic, Antarctic, and Alpine Research, **31**: 254. doi:10.2307/1552254.

Veraverbeke, S., Rogers, B.M., Goulden, M.L., Jandt, R.R., Miller, C.E., Wiggins, E.B., and Randerson, J.T. 2017. Lightning as a major driver of recent large fire years in North American boreal forests. Nature Climate Change, **7**: 529–534. doi:10.1038/nclimate3329.

Viereck, L.A., and Schandelmeier, L.A. 1980. Effects of fire in Alaska and adjacent Canada—a literature review. Technical Report 6, Bureau of Land Management — ADD 'BLM-Alaska Technical Report 6'. Fairbanks, AL.

Vincent, L.A., Zhang, X., Brown, R.D., Feng, Y., Mekis, E., Milewska, E.J., et al. 2015. Observed trends in Canada's climate and influence of low-frequency variability modes. Journal of Climate, **28**: 4545–4560. doi:10.1175/JCLI-D-14-00697.1.

Walker, X.J., Baltzer, J.L., Cumming, S.G., Day, N.J., Ebert, C., Goetz, S., et al. 2019. Increasing wildfires threaten historic carbon sink of boreal forest soils. Nature, **572**: 520–523. doi:10.1038/s41586-019-1474-y. PMID: 31435055.

Wein, R.W. 1976. Frequency and characteristics of Arctic Tundra fires. Arctic, **29**: 213–222. doi:10.14430/arctic2806.

Wein, R.W., and Bliss, L.C., 1973. Changes in Arctic *Eriophorum* Tussock communities following fire. Ecology, **54**: 845–852.

Wilcox, R.R. 1998. A note on the Theil-Sen regression estimator when the regresser is random and the error term is heteroscedastic. Biometrical Journal, **40**: 261–268. doi:10.1002/(SICI)1521-4036(199807)40:3⟨261::AID-BIMJ261⟩3.0.CO;2-V.

Yeung, C.A., and Li, R. 2018. Comparison of vegetation regeneration after wildfire between Mediterranean and tundra ecosystems by using Landsat images. Annals of GIS, **24**: 99–112. doi:10.1080/19475683.2018.1424740.

Young, A.M., Higuera, P.E., Duffy, P.A., and Hu, F.S. 2017. Climatic thresholds shape northern high-latitude fire regimes and imply vulnerability to future climate change. Ecography, **40**: 606–617. doi:10.1111/ecog.02205.

Zasada, J. 1986. Natural regeneration of trees and tall shrubs on forest sites in interior Alaska. Edited by K. Van Cleve, F.S. Chapin, P.W. Flanagan, L.A. Viereck and C.T. Dyrness. Forest Ecosystems in the Alaskan Taiga. Ecological Studies, **Vol. 57**, Springer, New York, NY.

Zhang, J., and Walsh, J.E. 2006. Thermodynamic and hydrological impacts of increasing greenness in northern high latitudes. Journal of Hydrometeorology, **7**: 1147–1163. doi:10.1175/JHM535.1.